GSJ: Volume 11, Issue 4, April 2023, Online: ISSN 2320-9186
www.globalscientificjournal.com

SPATIAL AND TEMPORAL CHANGES OF URBAN HEAT ISLAND IN JOS METROPOLIS, PLATEAU STATE, NIGERIA

Saleh Elisha Usman[1], Boyi J. Mairiga[1], Hyelduku Aliyu Mwada[1], Ojih Samuel[1], Ponsah E. Gwamzhi[1]

[1]National Centre for Remote Sensing, NCRS Jos
{National Space Research and Development Agency, NASRDA. Nigeria}

Saleh Elisha Usman. +234 8036329290. E-mail: utsmanrestricted@gmail.com

KeyWords
LST, LULC, NDBI, NDVI, Spatial, Temporal, UHI.

ABSTRACT

The Jos Metropolis in Nigeria has been under the pressure of urban growth over the past few decades. The population increase coupled with developmental activities within the city has led to urbanization. This urbanization and conversion of natural landscape into anthropogenic structure has resulted to temperature variation between the urban areas and the surrounding open areas. Furthermore, the temperature variability represents human-urban and rural contrast, which is due to deforestation and converting natural land surface into impervious land due to the urbanization. This paper examined the spatio-temporal variations of Urban Heat Island in Jos metropolis, a phenomenon that occurs when the temperature of a city or urban area is higher than the surrounding rural area by analyzing the Land-Use and Land-Cover (LULC), the Land Surface Temperature (LST), Normalized Difference Vegetation Index (NDVI) and the Normalized Difference Built-up Index (NDBI) of the study area and how they affect the city. In the end, the study showed that the Spatio-temporal changes of LST within the metropolis was on an increase owing to the Rural-Urban migration in the city, due to the presence of commercial and industrial activities within the metropolis.

INTRODUCTION

Over the past decades, Jos city is under the pressure of urban growth (Adzandeh et al., 2015). The population increase coupled with developmental activities within the city has led to urbanization (Seifolddini & Mansourian, 2014). The fast growth of urban area and conversion of natural landscape into anthropogenic structure results in change of local atmosphere and elevated land surface temperature compared to the surrounding open areas (Kikon et al., 2016).

The temperature variability represents human-urban and rural contrast, which is due to deforestation and conversion natural land surface into impervious land due to the urbanization(Chakraborty et al., 2015).

Urban heat island (UHI) is a phenomenon that occurs when the temperature of a city or urban area is higher than the surrounding rural area. It is caused by the presence of large amounts of concrete and asphalt, which absorb and retain heat, and the lack of vegetation, which would otherwise cool the air. A systematic review of the literature on UHI has been conducted in order to better understand the factors that contribute to UHI intensity and magnitude.

One study found that different spatial and temporal factors can affect UHI intensity and magnitude, such as urbanization, economic development, and population concentration (Deilami et al., 2018). Another study conducted a literature review of UHI intensity, focusing on international efforts to improve urban microclimate, minimize building energy consumption, and improve air quality (Tzavali et al., 2015). A third study conducted a systematic literature review (SLR) of 51 studies to assess the spatial extent of UHIs, the UHI concept used for UHI estimation, and the UHI estimation and analysis methods (Kim & Brown, 2021). Finally, a review of the current literature on UHI modeling was conducted to assess the current modeling capabilities for determining the impacts of UHI on outdoor comfort levels and urban building energy demands (Ameer & Krarti, 2022).

In Nigeria, research has been conducted to gain insights on the UHI phenomenon in medium-sized cities such as Akure (Popoola et al., 2020) and Kano (Umar & Kumar, 2014). Studies have shown that the UHI effect can have a significant impact on the health of people living in urban areas (Sunday, 2020), leading to issues such as depression, restlessness, heat rashes, sleeplessness, and even death. Additionally, research has been conducted to investigate the spatial and temporal changes of UHI in Kano Metropolis (Yang et al., 2016), as well as the effect of urbanisation on the occurrence of UHI over Kano Metropolis (Yahaya & Suleiman, 2017).

Research on urban heat islands is significant because it can help to better understand the impacts of climate change on public health and energy consumption, as well as inform climate adaptation policies.

As the planet warms, urban heat islands will only intensify those higher temperatures, making it increasingly important to find ways to alleviate them (EPA, 2019). Additionally, since nearly 70% of humanity will live in cities by 2050 (MIT, 2021), understanding the effects of urban heat islands on health is also critical.

Research has shown that urban heat islands can have a variety of impacts on health, including increased risk of heat-related illnesses, air pollution, and other health issues (Heaviside, 2020).

The aim of this study examines the spatio-temporal variations of UHI in Jos metropolis, Nigeria.

The following objectives are to be derived;

i. Spatial analysis of the Land-use and Land-cover of the Study area

ii. Spatial analysis of Land surface temperature, Normalized Difference Vegetation Index (NDVI), and Normalized Differential Built-Up Index (NDBI).

iii. Comparism of all three criteria's and how they affect the city.

Study Area

Jos is a city located in the north central region of Nigeria. It is the administrative capital and largest city of Plateau State. The city has a population of about 900,000 residents based on the 2006 census (Aliyu et al., 2019)[13]. The Jos Plateau is a plateau located near the center of Nigeria and gives its name to the Plateau State in which it is found [14]. It is composed of eroded gneiss formations, with granite intrusions forming massifs, and has numerous extinct volcanic cones surrounded by basaltic flows, especially around Panyam in the south and around Vom and Miango in the west, including several containing crater lakes (Aliyu et al., 2019). Plateau State is celebrated as "The Home of Peace and Tourism". It has an area of 291 km² and a population of 429,300 at the 2006 census. The languages spoken in Jos are Anaguta, Afizere & Berom (Muhammad-Bashir et al., 2016). it has an average elevation of 1263.05 meters (4143.86 feet) above sea level. It has a tropical wet and dry or savanna climate (classified as Aw) with an average yearly temperature of 28.41ºC (83.14ºF) and an average minimum and maximum temperature of 16-26°C. The climate of Jos Plateau is dominantly influenced by its relatively high altitude and position along the Inter Tropical Convergence Zone (ITCZ) (Solomon Zi & Hyacinth M, 2020).

The climate of Jos Plateau is characterized by a cool rainy climate and its numerous rivers, including the Kaduna, Karami, and N'gell, which feed the Niger River; the Mada, Ankwe, Dep, Shimanker, and Wase, which flow to the Benue; the Lere, Maijuju, and Bagei, which supply the Gongola; and the Kano, Delimi, Bunga, Jamaari, and Misau, which intermittently nourish the area (Solomon Zi & Hyacinth M, 2020).

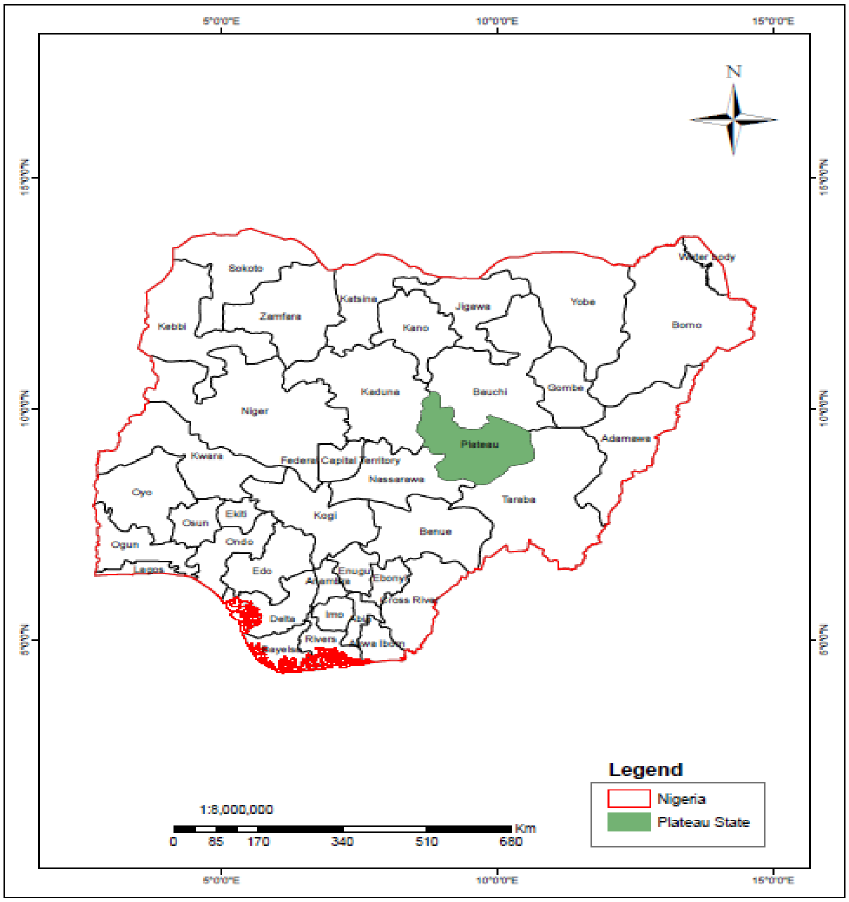

Fig 1: Nigeria map Showing Plateau State

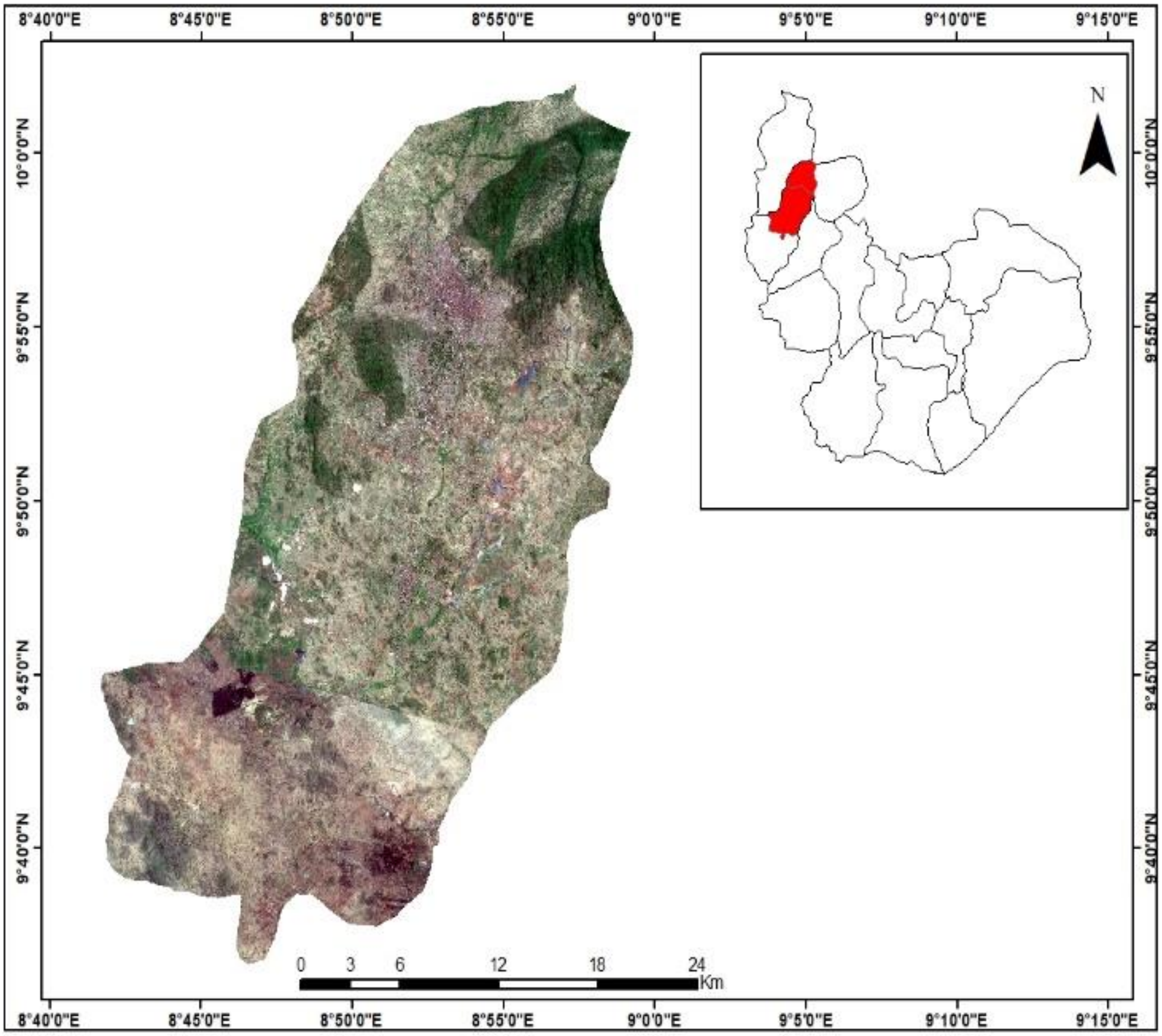

Fig. 2: True color Sentinel-2A image of the Study Area

Data Used: Satellite Data

The details of satellite images used in this study are given in Table 1.

Table 1: Data Used and their sources

Data Used	Acquisition Date	Source of Data
LandSat-7 ETM+	6th February,2002	http://earthexplorer.usgs.gov
LandSat-7 ETM	13th December,2010	http://earthexplorer.usgs.gov

LandSat-8 OLI	12th January, 2019	http://earthexplorer.usgs.gov

Image Analysis and Land Surface Temperature Estimation

The Land Surface Temperature (LST) can be accurately measured using images from Landsat sensors. This is because the thermal bands of Landsat images capture the LST of the terrestrial surface, allowing for a detailed analysis of how urban heat islands are formed.

By analyzing and comparing the thermal bands of Landsat images, we can estimate the intensity of an urban heat island in a given area. The process begins with pre-processing the images by calibrating and radiometrically correcting them, followed by atmospheric correction to reduce errors caused by veiling haze and aerosols.

Then, a temperature regression model must be built by applying linear regression equations to the thermal bands. The results are plotted on a graph to determine the temperature coefficient (TC) and gradient (G). The TC and G are then used to calculate an overall urban heat index for Jos, Plateau State using an equation created specifically for this purpose.

Finally, image segmentation is used to classify land cover with either high or low TC coefficients. this helps determine how much or how little of an urban heat island effect has occurred in the area. With this information, we can gain valuable insights into why temperatures may be higher in some areas than others.

Pre-Processing

Preprocessing of Landsat images involves several steps to prepare the data for analysis. These steps typically include:

1. Radiometric calibration: The raw digital numbers (DN) from Landsat sensors need to be converted to radiance values. This is done using calibration coefficients provided by the USGS.
2. Atmospheric correction: The radiance values can be affected by atmospheric conditions, so atmospheric correction is necessary to remove these effects. This involves estimating the atmospheric properties and removing the atmospheric effects from the image.
3. Geometric correction: Landsat images may have distortions due to its position. Geometric correction involves correcting these distortions

and aligning the images to a standard coordinate system.

4. Mosaicking: Landsat images are often acquired in multiple scenes that need to be combined into a single image. Mosaicking involves selecting the best pixels from each scene and combining them into a seamless image.

5. Subset and resample: Landsat images can cover large areas, so it may be necessary to subset the image to a smaller area of interest. Additionally, the resolution of the image may need to be resampled to match the resolution of other data layers.

These pre-processing steps are essential for ensuring that Landsat data is reliable and accurate for subsequent analysis, such as land cover classification or land surface temperature estimation.

METHODOLOGY USED

Conversion to Radiance

Any object with a temperature above absolute zero Kelvin emits thermal electromagnetic energy. The signals received by the thermal sensors of Landsat TM/ETM+ are stored and represented as digital numbers (DN). (Oguz, 2013) In order to convert the Digital number of the Landsat 7 ETM and Landsat 8 OLI into Spectral Radiance the following equation was inputted into ARCMAP 10.5.

a) **For Landsat 7**

$$L\lambda = (\frac{LMAX\lambda - LMIN\lambda}{(QCALMAX - QCALMIN)}/(QCAL - QCALMIN) + LMIN\lambda$$

where:

m^2= meter squared

Lλ = Spectral Radiance at the sensor's aperture in watts/ (m^2 * ster * μm)

QCAL = the quantized calibrated pixel value in DN

LMINλ = the spectral radiance that is scaled to QCALMIN in watts/ (m^2 *ster* μm)

LMAXλ = the spectral radiance that is scaled to QCALMAX in watts/ (m^2*ster * μm)

QCALMIN = the minimum quantized calibrated pixel value (corresponding to LMINλ) in DN

QCALMAX = the maximum quantized calibrated pixel value (corresponding to LMAXλ) in DN=

255

b) **For Landsat 8**

These values can then be converted to spectral radiance using the radiance scaling factors provided in the metadata file.

Lλ = ML*Qcal + AL

where:

Lλ = Spectral radiance (W/ (m2 * ster * μm))

ML = Radiance multiplicative scaling factor for the band (RADIANCE_MULT_BAND_n from the metadata).

AL = Radiance additive scaling factor for the band (RADIANCE_ADD_BAND_n from the metadata).

Qcal = Level 1-pixel value in DN (Oguz, 2013)

Conversion to Temperature

Any object with a temperature above absolute zero Kelvin emits thermal electromagnetic energy. The signals received by the thermal sensors of Landsat TM/ETM+ are stored and represented as digital numbers (DN). Any object with a temperature above absolute zero Kelvin emits thermal electromagnetic energy. The signals received by the thermal sensors of Landsat TM/ETM+ are stored and represented as digital numbers (DN).

Spectral radiance can also be converted to brightness temperature, which is the effective temperature viewed by the satellite under an assumption of unity emissivity. The conversion formula is:

$$T = \frac{K2}{\ln\left(\frac{K1}{L_\lambda} + 1\right)}$$

where:

T = Top of Atmosphere Brightness Temperature, in Kelvin.

Lλ = Spectral radiance (Watts/(m2*ster*µm))

K1 = Thermal conversion constant for the band (K1_CONSTANT_BAND_n from the metadata)

K2 = Thermal conversion constant for the band (K2_CONSTANT_BAND_n from the metadata)

Land Surface Temperature

The brightness temperatures from TM band 6 thermal were then used to calculate the land surface temperature using the Sobrino equation (Sobrino et al., 2004).

$$Ts = BT/(1+ (W \times BT/p)\ln e$$

where:

Ts = land surface temperature

BT = at-sensor brightness temperature (K)

W = wavelength of emitted radiance (11.5um);

ln *e* = Log of the spectral emissivity value

NDVI and NDBI Derivation:

Different ground indices such as Normalized Difference Vegetation Index (NDVI) and Normalized Difference Built-up Index (NDBI) were selected for further analyzing relationship between UHIs and green cover land by calculating and analyzing the UHIs-VIs profiles and the spatial distributions of LST profiles. For Landsat ETM+ data. The equation is given below

$$NDVI = (NIR - RED) / (NIR + RED)$$

Where:

NIR band represents Band 4 in Landsat TM (0.76–0.90 _m (wavelength)) and Band 5 in Landsat OLI (0.85–0.88 _m (wavelength)) respectively,

RED band represents Band 3 in Landsat TM (0.63–0.69 _m (wavelength)) and Band 4 in

Landsat OLI (0.64–0.67 _m (wavelength)), respectively.

Calculation of land surface emissivity

Land surface emissivity (LSE) is the average emissivity of an element of the surface of the Earth which can be derived from the equation below

$$PV = [(NDVI - NDVI\ min) / (NDVI\ max + NDVI\ min)] ^\wedge 2$$

Where:

PV = Proportion of Vegetation

NDVI = DN values from NDVI Image

NDVI min = Minimum DN values from NDVI Image

NDVI max = Maximum DN values from NDVI Image

$$i = 1.0094 + 0.0047 \ln(PV)$$

Where:

i = Land Surface Emissivity

PV = Proportion of vegetation

Land Surface Temperature (LST) for Landsat 8 band 10 can be calculated using

$$LST = (BT / 1) + W * (BT / 14380) * \ln(i)$$

Where:

BT = Top of atmosphere brightness temperature (°C)

W = Wavelength of emitted radiance

i = Land Surface Emissivity

RESULTS AND DISCUSSIONS

Spatio-temporal Analysis of the Land Cover

Jos metropolitan was classified into six classes waterbody, Built-up, Degraded Land, Farmland, Rock-Outcrop and Vegetation. Three different periods were considered (2002, 2010, and 2019) with an interval of 17 years between the first year and the final year in-order to depict the changes within the metropolis over the course of the years.

It shows that degraded land increased the most, which increased from 35 km^2 (4.23%) in 2002 to 46 km^2 (5.56%) in 2010 to 261 km^2 (31.52%) in 2019, this is as a result of the increment of mining activities within the area and it also had impact on the built-up which raised from 28 km^2 (3.38%) in 2002 to 99 km^2 (11.96%) in 2010 to 140 km^2 (16.91%) in 2019, the urbanization of the study area saw a great decline in the agricultural activities in the area with farmlands which covers 621 km^2 (75%) in 2002 to 426 km^2 (51.45%) to a further low of 287 km^2 (34.66%) in 2019. Also, due to the presence of mines it also led to a partial increase of mine ponds in the southern part 121 km^2 (14.61%) 2002 to 223 km^2 (26.93%) but later a sharp decline due to the ponds being drained for Construction and agricultural purposes and most within the northern region converted into settlements. Also, due to shift in Ecological laws in the state the Vegetative zones had a brief increase 13 km^2 (1.57%) 2002 to 20Sqkm (2.42%) 2010 but a change of the laws within the years also resulted into a decrease 17 km^2 (2.05%) in 2019, rock outcrop increased from 10 km^2 (1.21%) in 2002 to 14 km^2 (1.69%) and to a further 15 km^2 (1.81%) which is as a result of deforestation within the montane vegetation. (fig3, table2)

Table2: statistics of LULC classification for 2002, 2010, and 2019

	2002		2010		2019	
LULC	Area (Km^2)	(%)	Area (Km^2)	(%)	Area (Km^2)	(%)
Built Up	28	3.38	99	11.96	140	16.91
Degraded Land	35	4.23	46	5.56	261	31.52
Farm Land	621	75.00	426	51.45	287	34.66
Rock Outcrop	10	1.21	14	1.69	15	1.81
Vegetation	13	1.57	20	2.42	17	2.05
Waterbody	121	14.61	223	26.93	108	13.04

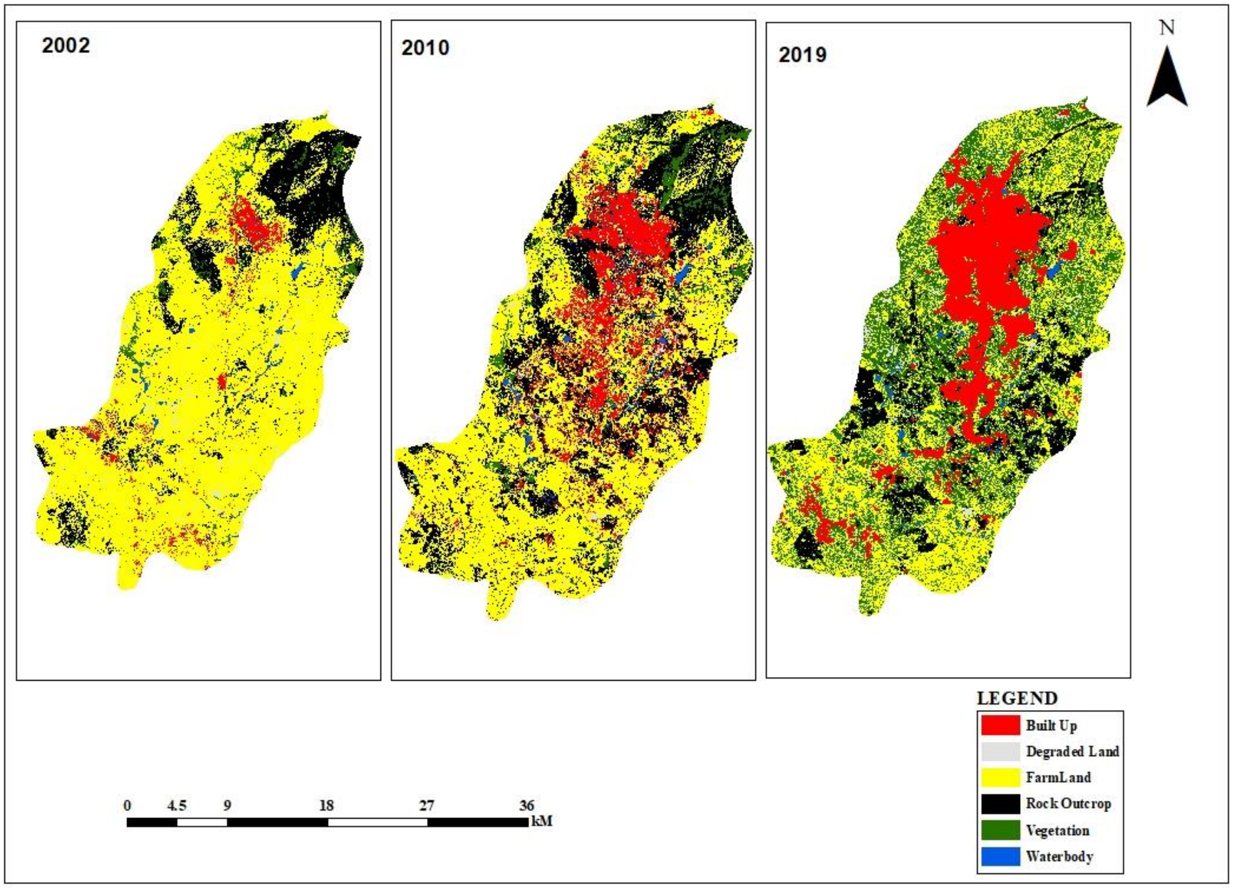

Figure 3: LULC classification of the Jos_Bukuru Metropolis for 2002, 2010, and 2019

Spatio-Temporal Analysis of Land Surface Temperature

In this study, calculations of urban heat island intensity in Jos, Plateau State Nigeria were studied. The analysis was performed using Landsat images. The results showed that the maximum land surface temperature was 43^{0}C (2002), 46.15^{0}C (2010), and 43.16^{0}C (2019) while the minimum land surface temperature was 16.54^{0}C (2002), 17.44^{0}C (2010), and 17.43^{0}C (2019). indicating an average deviation temperature of 13.48^{0}C and an average temperature of 30.62^{0}C in Jos.

Table3: land surface temperature distribution within the given years.

Year	Min	Max	Average	Avedev
2002	16.54	43	29.77	13.23
2010	17.44	46.15	31.795	14.355
2019	17.43	43.16	30.295	12.865

			30.62	13.48333

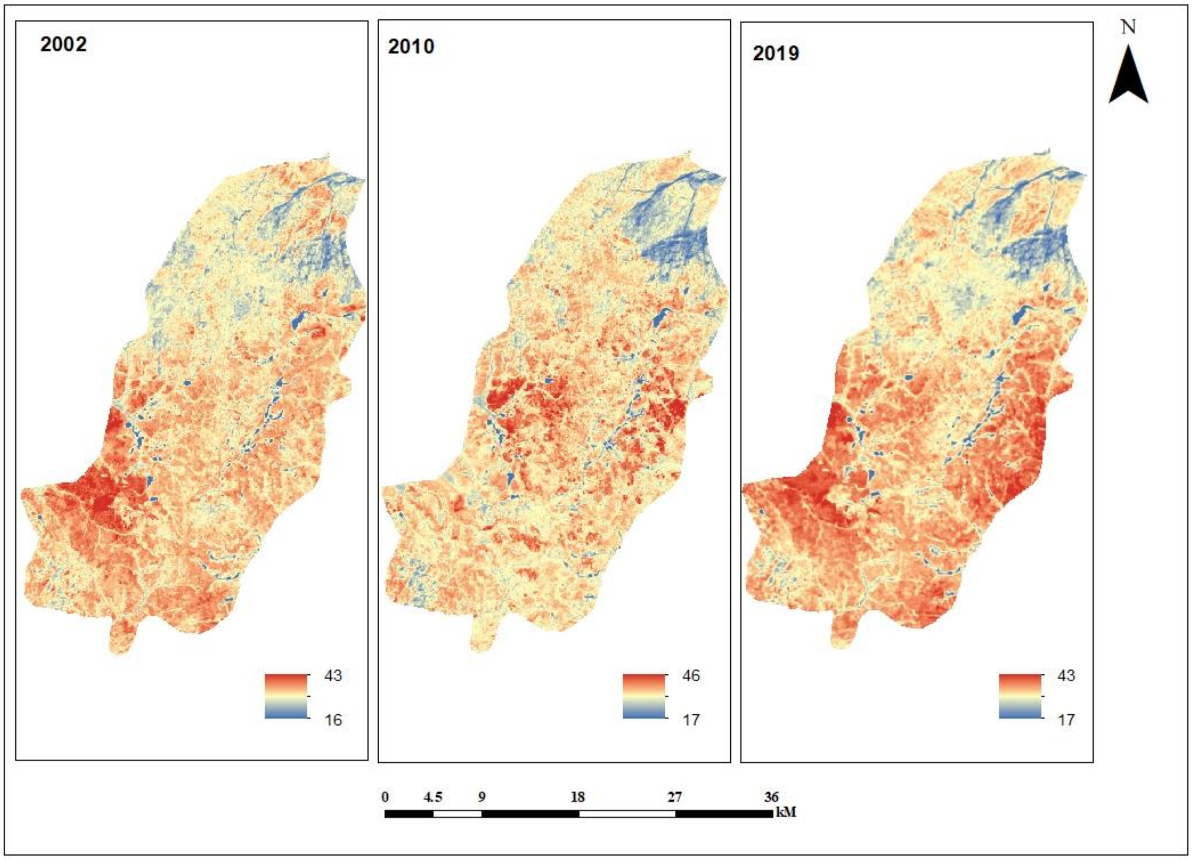

Figure4: LST distribution within Jos Metropolis between 2002, 2010 and 2019.

Spatio-temporal analysis NDBI

The Spatio-temporal distribution of NDBI in Jos metropolis **(figure)** for the years 2002, 2010, and 2019 shows that the average NDBI value was observed to be 0.135 in 2002, which decreased to -0.045 in 2010 and further increased to 0.175 in 2019 **(table)**. the decrease in 2010 was as a result of communal clashes in the metropolis in 2010, which properties were largely destroyed.

The distribution of NDBI can be seen to be located in the central and upper part of the city which makes up the large part of the metropolis due to its built-up and commercial activities. While low NDBI is found in the southern part of the city due to its agricultural practices and vegetation conservation.

Table 4: NDBI distribution within the given years.

Year	Min	Max	Average
2002	-0.28	0.55	0.135

2010	-0.96	0.87	-0.045
2019	-0.3	0.65	0.175

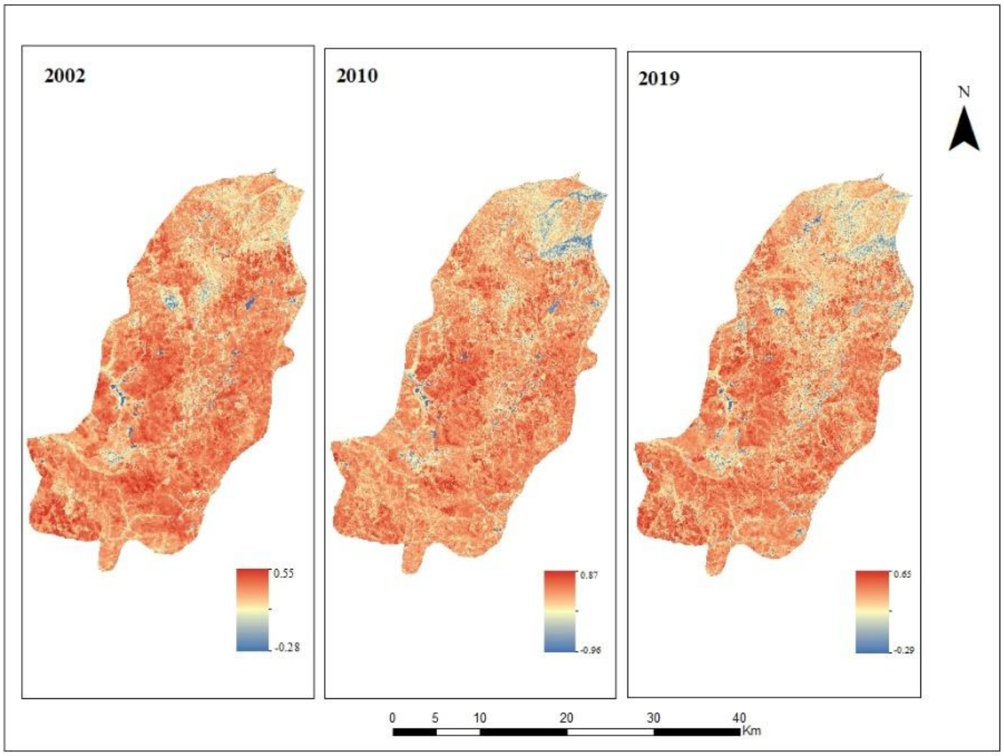

Figure 5: NDBI distribution within Jos Metropolis between 2002, 2010 and 2019.

Spatio-temporal analysis of NDVI

The spatial distribution of NDVI from Landsat image for the years 2002, 2010 and 2019 in Jos Metropolis is shown in Table 3. The minimum and maximum NDVI values of 2002 are in the range between −0.6 and 0.06 and during 2010, the range was between −0.74 and 0.44 and that of 2019 range between -0.29 and 0.40. It was observed that with the growth in urbanization, the vegetations around the urban centres decreased.

Table 5: NDVI distribution within the given years.

Year	Min	Max	Average
2002	-0.6	0.06	-0.27
2010	-0.74	0.44	-0.15
2019	-0.29	0.4	0.055

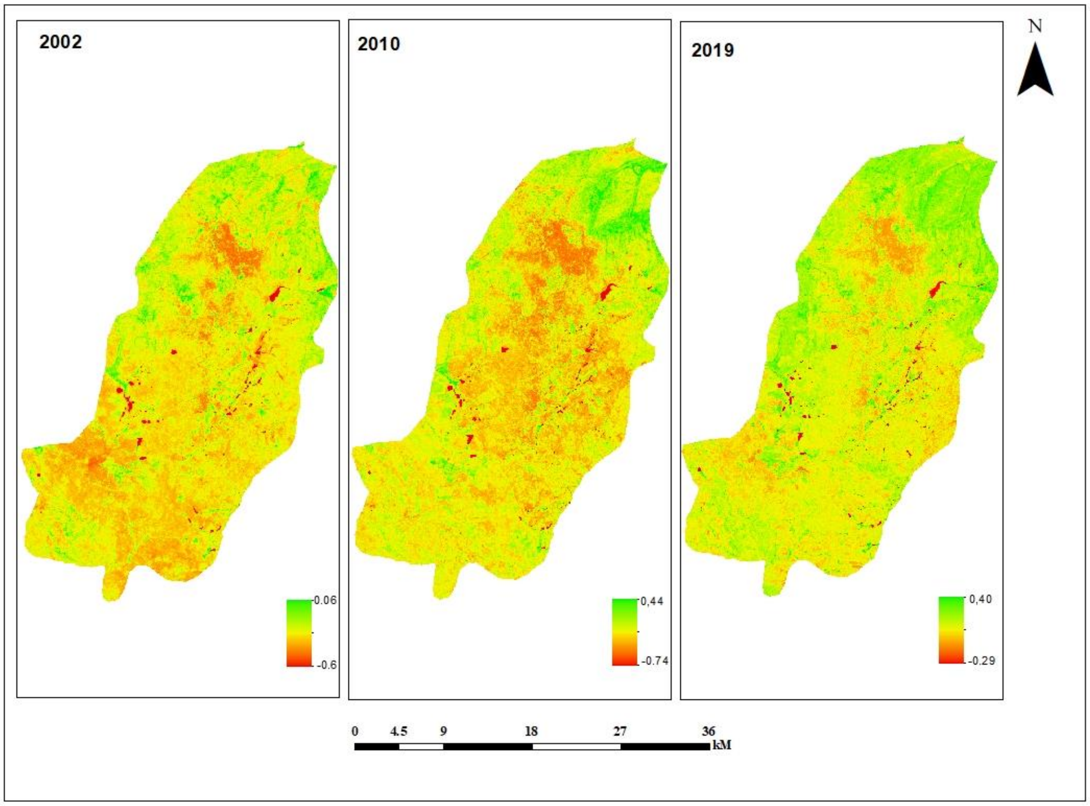

Figure 6: NDVI distribution within Jos Metropolis between 2002, 2010 and 2019

CONCLUSION

The result from the study showed that the Spatio-temporal changes of LST within the metropolis is on an increase and this is because of the Rural-Urban migration in the city, due to the presence of commercial and industrial activities within the metropolis.

Urban heat island mitigation strategies can be divided into five main categories: increasing tree and vegetative cover, installing green roofs, installing cool roofs, using cool pavements, and utilizing smart growth practices.

1. Increasing tree and vegetative cover can help reduce the urban heat island effect by providing shade and cooling the air through evapotranspiration.
2. Green roofs are also an effective strategy for reducing the urban heat island effect, as they provide both direct and ambient cooling effects and improve air quality.
3. Cool roofs are reflective and can help reduce the amount of heat absorbed by the building and the surrounding area.
4. Cool pavements, such as reflective or permeable pavements, can also help reduce the urban heat island effect.
5. Finally, utilizing smart growth practices, such as compact development and mixed land use, can help reduce the urban heat island effect.

ISSN 2320-9186

References

[1] Adzandeh, E. A., Akintunde, J. A., & Akintunde, E. A. (2015). *Analysis of urban growth agents in Jos metropolis, Nigeria*.

[2] Aliyu, A., Abdulyakeen, K., Belel, S., Babanyara, Y., Salis, A., Ibrahim, A., & Is'haq, D. (2019). Heavy Metals in Water and Plants along Rivers Dilimi and Jenta, Jos. Plateau State, Nigeria. *American Journal of Engineering Research*, *8*(3), 32–38.

[3] Ameer, B., & Krarti, M. (2022). Review of Urban Heat Island and Building Energy Modeling Approaches. *Journal of Engineering for Sustainable Buildings and Cities*, *3*(1), 011003.

[4] Chakraborty, S. D., Kant, Y., & Mitra, D. (2015). Assessment of land surface temperature and heat fluxes over Delhi using remote sensing data. *Journal of Environmental Management*, *148*, 143–152.

[5] Deilami, K., Kamruzzaman, M., & Liu, Y. (2018). Urban heat island effect: A systematic review of spatio-temporal factors, data, methods, and mitigation measures. *International Journal of Applied Earth Observation and Geoinformation*, *67*, 30–42.

[6] Heaviside, C. (2020). *Urban Heat Islands and Their Associated Impacts on Health*. Oxford University Press.

Kikon, N., Singh, P., Singh, S. K., & Vyas, A. (2016). Assessment of urban heat islands (UHI) of Noida City, India using multi-temporal satellite data. *Sustainable Cities and Society*, *22*, 19–28.

[7] Kim, S. W., & Brown, R. D. (2021). Urban heat island (UHI) intensity and magnitude estimations: A systematic literature review. *Science of the Total Environment*, *779*, 146389.

[8] Muhammad-Bashir, B., Sani, A. M., Ademola, O. P., Peterside, K., Maryam, M., & Jenna, F. (2016). Prevalence and demographic distribution of canine rabies in Plateau state, Nigeria, 2004–2009. *Animal Health and Production*, *64*(1), 127–136.

[9] Oguz, H. (2013). LST calculator: A program for retrieving land surface temperature from Landsat TM/ETM+ imagery. *Environmental Engineering and Management Journal*, *12*(3), 549–555.

[10] Popoola, O., Durojaye, P., Bayode, T., Popoola, A., Olanibi, J., & Aladetuyi, O. (2020). Spatio-temporal variance and urban heat island in Akure, Nigeria: A time-spaced analysis Using GIS Techniqu. *South African Journal of Geomatics*, *9*(2), 365–378.

[11] Seifolddini, F., & Mansourian, H. (2014). Spatial-temporal pattern of urban growth in Tehran Megapole. *Journal of Geography and Geology*, *6*(1), 70.

[12] Sobrino, J. A., Jiménez-Muñoz, J. C., & Paolini, L. (2004). Land surface temperature retrieval from LANDSAT TM 5. *Remote Sensing of Environment*, *90*(4), 434–440.

[13] Solomon Zi, W., & Hyacinth M, D. (2020). Climate Change, Rainfall Trends and Variability in Jos Plateau. *Journal of Applied Sciences*, *20*(2), 76–82.

[14] Sunday, I. (2020). ASSESSMENT OF URBAN GENERATED CLIMATE ANOMALY IN OKENE TOWN, OKENE LOCAL GOVERNMENT AREA OF KOGI STATE, NIGERIA. *FUDMA JOURNAL OF SCIENCES*, *4*(2), 101–110.

[15] Tzavali, A., Paravantis, J. P., Mihalakakou, G., Fotiadi, A., & Stigka, E. (2015). Urban heat island intensity: A literature review. *Fresenius Environmental Bulletin*, *24*(12b), 4537–4554.

[16] Umar, U. M., & Kumar, J. S. (2014). Spatial and temporal changes of urban heat island in Kano Metropolis, Nigeria. *Int J Res Eng Sci Technol*, *1*, 1–9.

[17] Yahaya, T. I., & Suleiman, Y. M. (2017). *Urbanisation Effect on the Occurrence of Urban Heat Island over Kano Metropolis, Nigeria*.

[18] Yang, L., Qian, F., Song, D.-X., & Zheng, K.-J. (2016). Research on urban heat-island effect. *Procedia Engineering*, *169*, 11–18.